Supplementary Materials for

Real-time imaging of accelerated solid-liquid-gas reactions with nanobubbles

Wen Wang[1,2,†], Tao Xu[1,†], Jige Chen[3,6,†], Junyi Shangguan[2,5], Hui Dong[7], Huishu Ma[6], Qiubo Zhang[2], Tingting Bai[8], Zhirui Guo[8], Haiping Fang[4]*, Haimei Zheng[2,5,*] & Litao Sun[1,*]

[1] SEU-FEI Nano-Pico Center, Key Laboratory of MEMS of Ministry of Education, Collaborative Innovation Center for Micro/Nano Fabrication, Device and System, Southeast University, Nanjing, 210096, China.

[2] Materials Sciences Division, Lawrence Berkeley National Laboratory, Berkeley, CA 94720, USA.

[3] Shanghai Synchrotron Radiation Facility, Zhangjiang Laboratory, Shanghai Advanced Research Institute, Chinese Academy of Sciences, Shanghai, 201204, China.

[4] Department of Physics, East China University of Science and Technology, Shanghai 200237, China.

[5] Department of Materials Science and Engineering, University of California, Berkeley, California 94720, USA.

[6] Shanghai Institute of Applied Physics, Chinese Academy of Sciences, Shanghai 201800, China.

[7] Key Laboratory of Welding Robot and Application Technology of Hunan Province, Engineering Research Center of Complex Tracks Processing Technology and Equipment of Ministry of Education, Xiangtan University, Xiangtan 411105, China.

[8] The Second Affiliated Hospital, Key Laboratory for Aging & Disease, Nanjing Medical University, Nanjing 210011, P. R. China.

*Correspondence to: slt@seu.edu.cn (L.S.); hmzheng@lbl.gov (H.Z.) and fanghaiping@sinap.ac.cn (H.F.).

†Contributed equally to this work

Supplementary Materials:

Supplementary Figures and Figure Captions 1 to 15

Supplementary Videos Captions 1 to 4

Other Supplementary Materials include the following:

Supplementary Videos 1 to 4

Video Captions

Supplementary Video 1. The uniform etching of a Au nanorod without nanobubble. The electron dose rate was 780 $e^-/Å^2 \cdot s$.

Supplementary Video 2. The etching of a Au nanorod with nanobubbles at the side. The electron dose rate was 370 $e^-/Å^2 \cdot s$.

Supplementary Video 3. The etching of a Au nanorod with a nanobubble at one end. The electron dose rate was 370 $e^-/Å^2 \cdot s$.

Supplementary Video 4. The etching of a Au nanorod with moving nanobubbles. The electron dose rate was 200 $e^-/Å^2 \cdot s$.

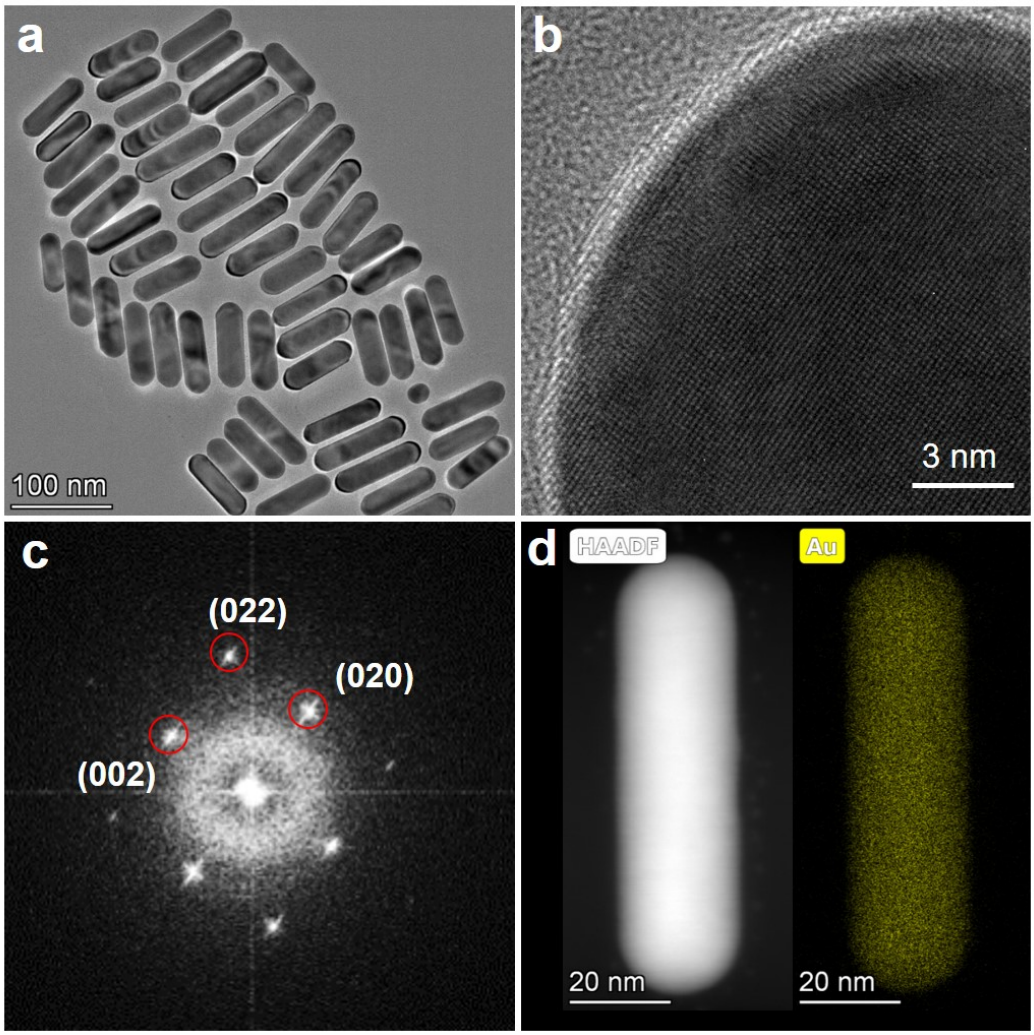

Supplementary Fig. 1. Characterization of the pristine Au nanorods before etching. a, Low magnification TEM image of the Au nanorods. **b**, Representative high resolution TEM of an Au nanorod. **c**, Fast Furrier transform (FFT) pattern of the image in **b**. **d**, STEM-EDS elemental mapping of an Au nanorod.

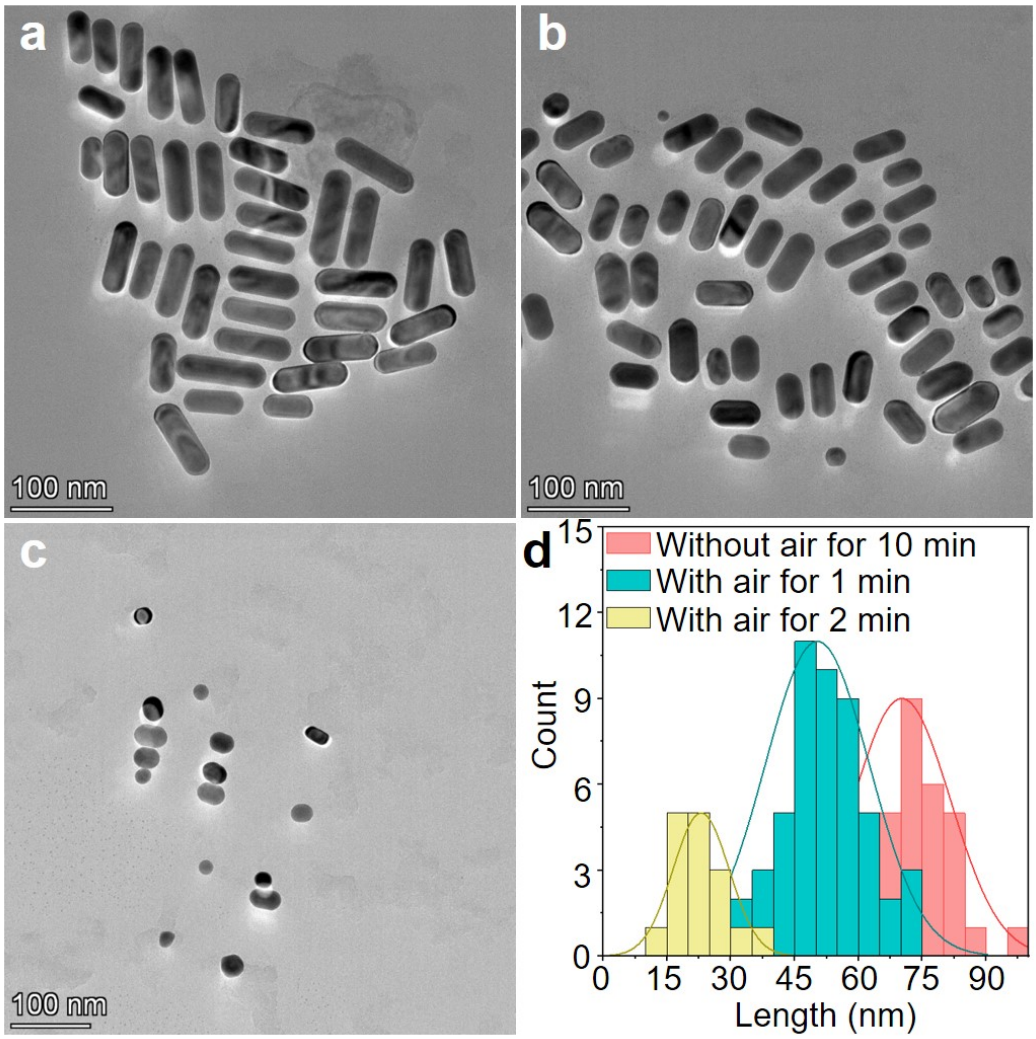

Supplementary Fig. 2. Etching of Au nanorods in air with and without bubbling air into the solution. a, A TEM image showing Au nanorods are stable in air for 10 min at 70 ºC without bubbling air into the solution. **b**,**c**, TEM images showing that Au nanorods are etched with bubbling air into the solution at 70 ºC for 1 and 2 min, respectively. The Au nanorod can be completely etched in HBr aqueous solution within a few minutes. **d**, Histograms of nanorod length distribution under different etching conditions.

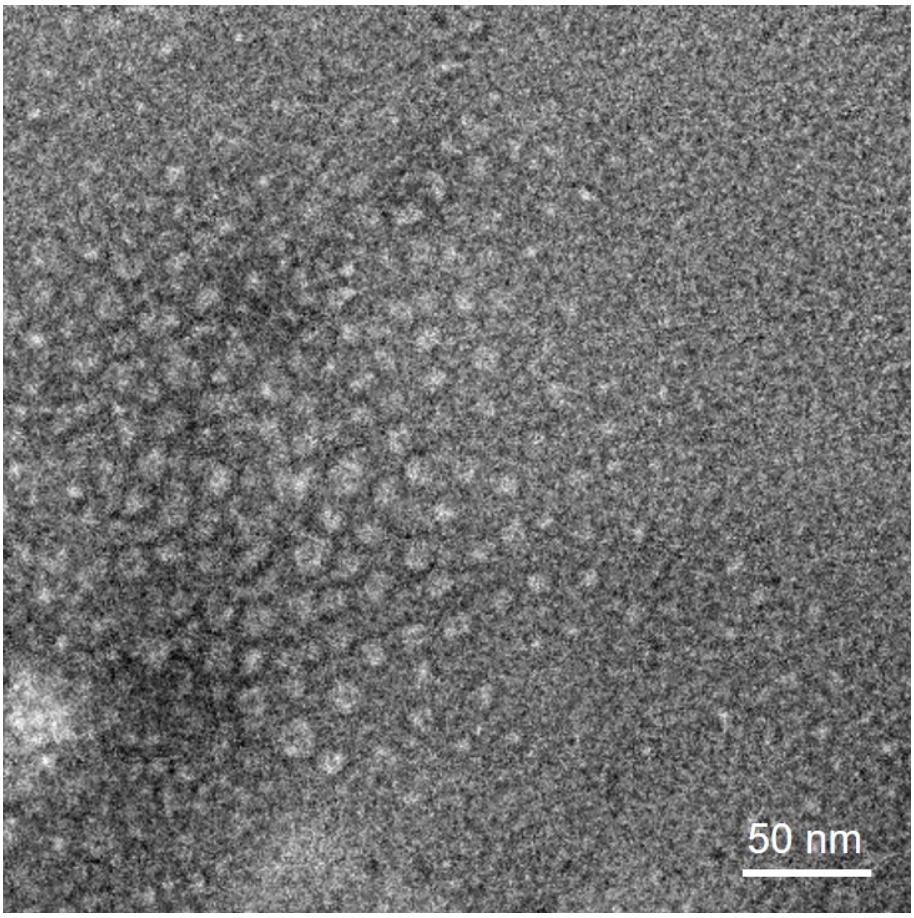

Supplementary Fig. 3. TEM image of the solution that is constantly bubbling after being illuminated with an extended period of time.

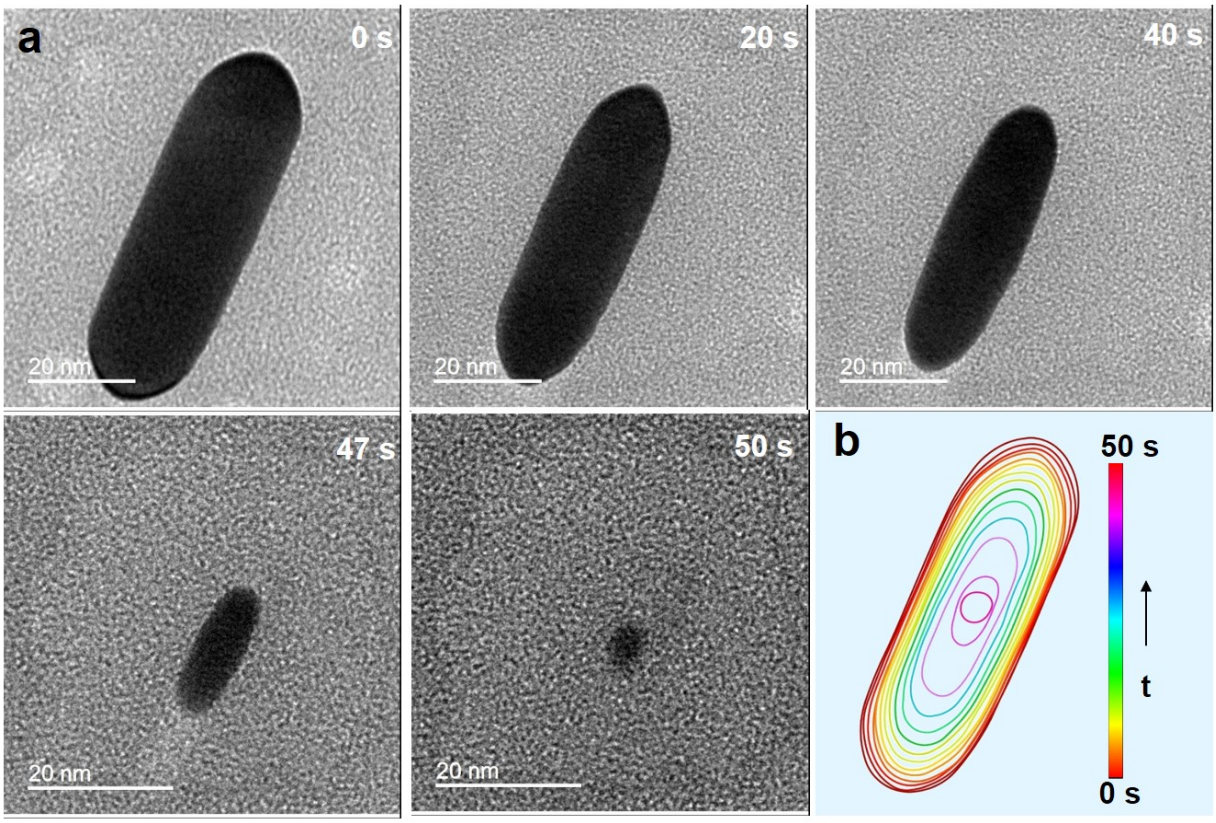

Supplementary Fig. 4. Uniform etching of a Au nanorod without gas nanobubbles in the near distance (also see Supplementary Video 1). **a**, Sequence of in situ TEM images showing the morphology changes of Au nanorod during etching without nanobubbles. **b**, Corresponding contour map highlighted the uniform shape evolution of the nanorod.

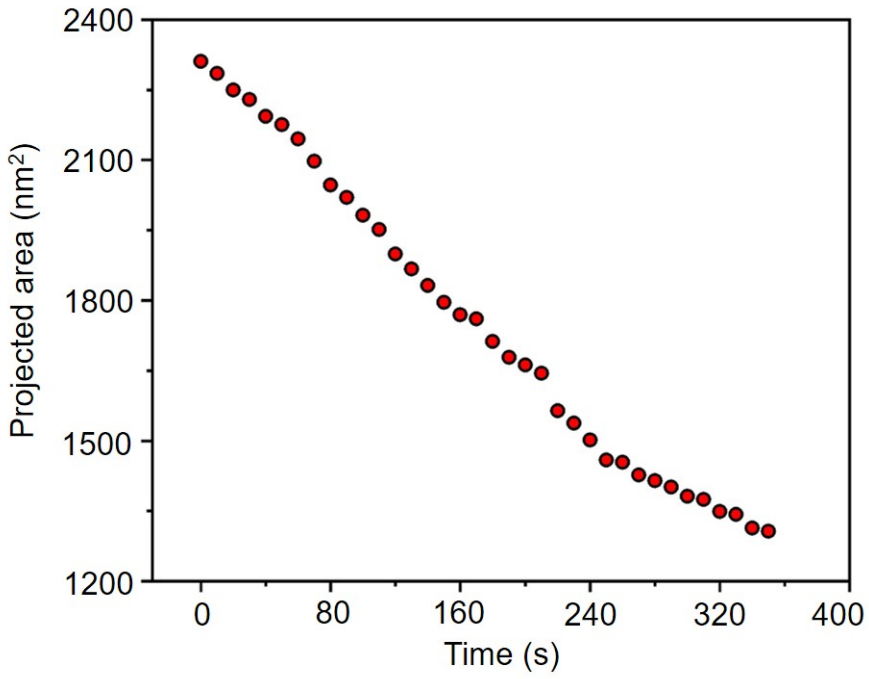

Supplementary Fig. 5. Plots of projected area of the nanorod as the function of time. The projected area of nanorod gradually decreases with time while the contrast of nanorod is uniform (Fig. 2 and Supplementary Video 2), which suggests the indented area is formed by the etching of nanorod rather than mass redistribution.

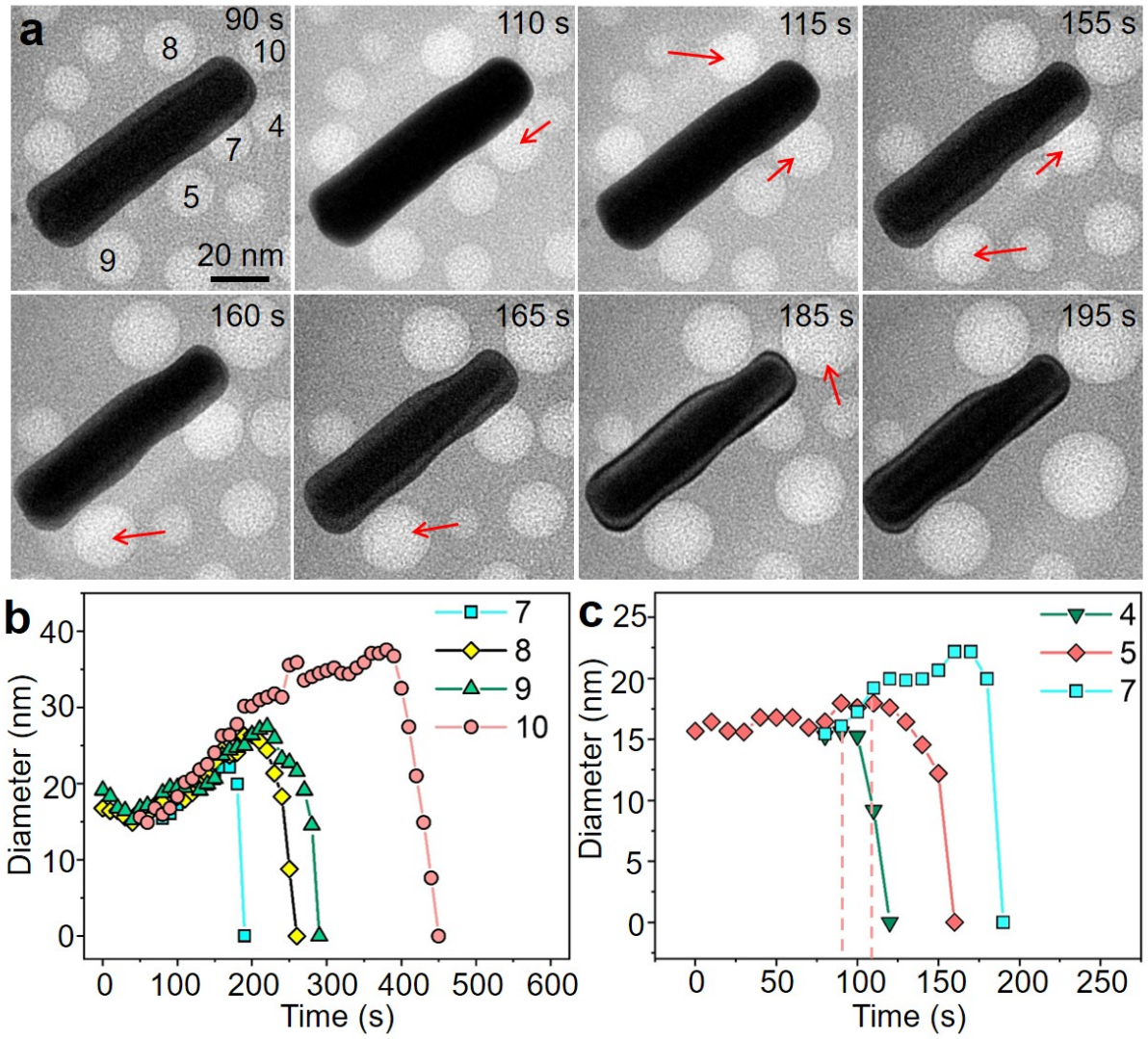

Supplementary Fig. 6. The growth of nanobubbles by Ostwald ripening. a, A sequence of in-situ TEM images showing the dynamic behavior of nanobubbles (also see Supplementary Video 1). Some nanobubbles grow by consuming other nanobubbles in a close distance. The red arrows represent the gas transfer directions between two adjacent nanobubbles. **b**, Diameter changes of nanobubbles with time. The numbers represent the different nanobubbles marked in **a**. **c**, Diameter changes of three neighboring nanobubbles with time. The nanobubble 7 grows through gas transfer between the two neighboring nanobubbles (4 and 5).

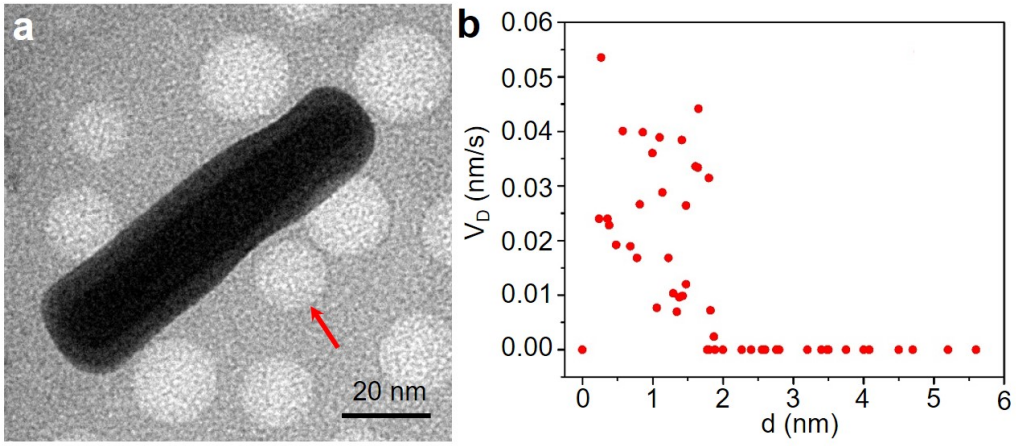

Supplementary Fig. 7. The local etching rate of a Au nanorod with nanobubbles nearby. a, A TEM image of nanorod with nanobubbles. **b**, Local transverse etching rate as a function of the distance between nanorod and the nanobubble marked by the red arrow in **a**.

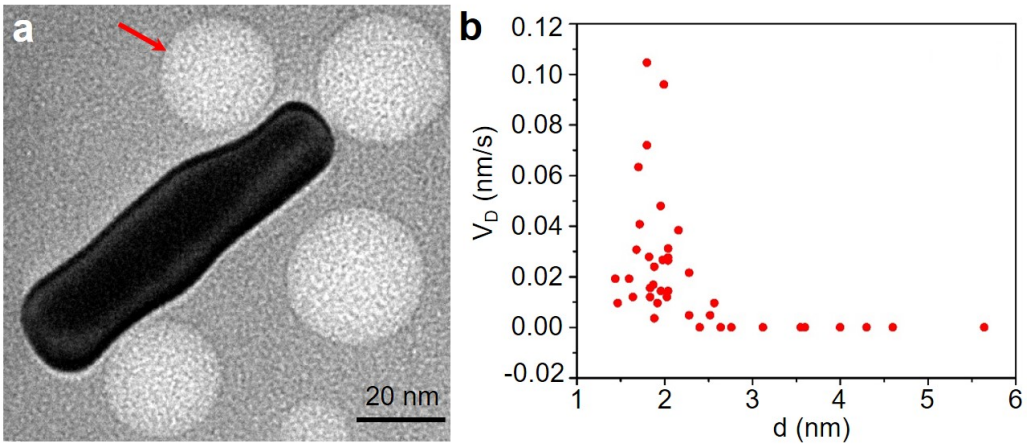

Fig. 8. The local etching rate of a Au nanorod with nanobubbles nearby. a, A TEM image of nanorod with nanobubbles. **b**, Local transverse etching rate as a function of the distance between nanorod and the nanobubble marked by the red arrow in **a**.

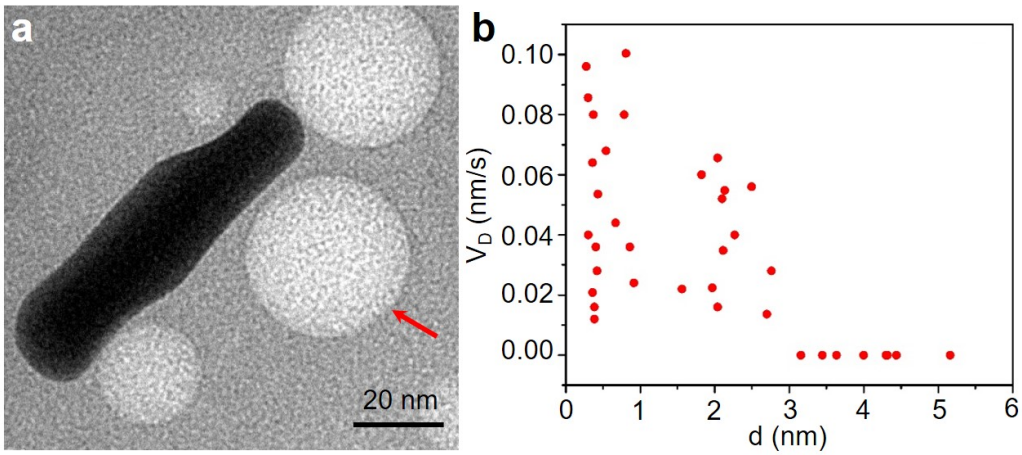

Supplementary Fig. 9. The local etching rate of a Au nanorod with nanobubbles nearby. a, A TEM image of nanorod with nanobubbles. **b**, Local transverse etching rate as a function of the distance between nanorod and the nanobubble marked by the red arrow in **a**.

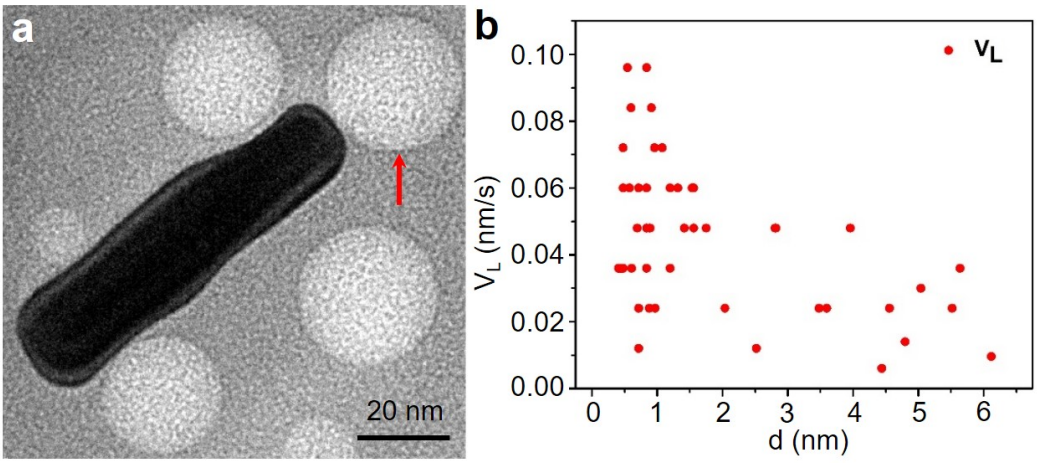

Supplementary Fig. 10. The local etching rate of a Au nanorod with nanobubbles nearby. a, A TEM image of nanorod with nanobubbles. **b**, Longitudinal etching rate as a function of the distance between nanorod and the nanobubble marked by the red arrow in **a**.

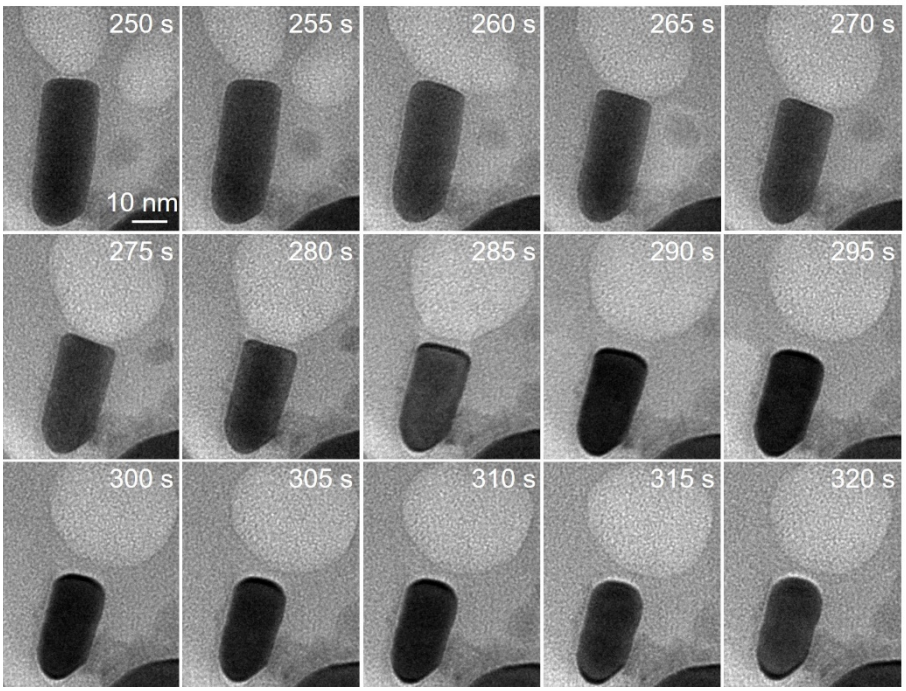

Supplementary Fig. 11. Time sequential TEM images showing the morphology evolution of a Au nanorod with a O_2 gas nanobubble at an end of nanorod.

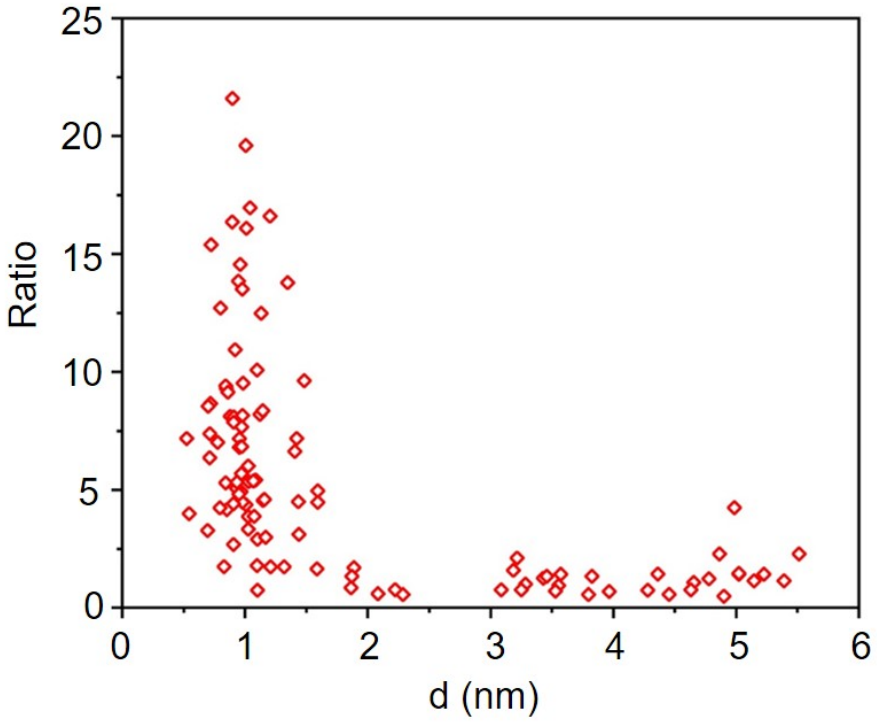

Supplementary Fig. 12. Ratio of the longitudinal etching rate for a Au nanorod with and without nanobubbles. The plot was achieved by measuring the longitudinal etching rate as a function of the distance between the Au surface and nanobubble (Fig. 3). And, all the values divided by the average longitudinal etching rate without a nanobubble during the early stage (0-150 s).

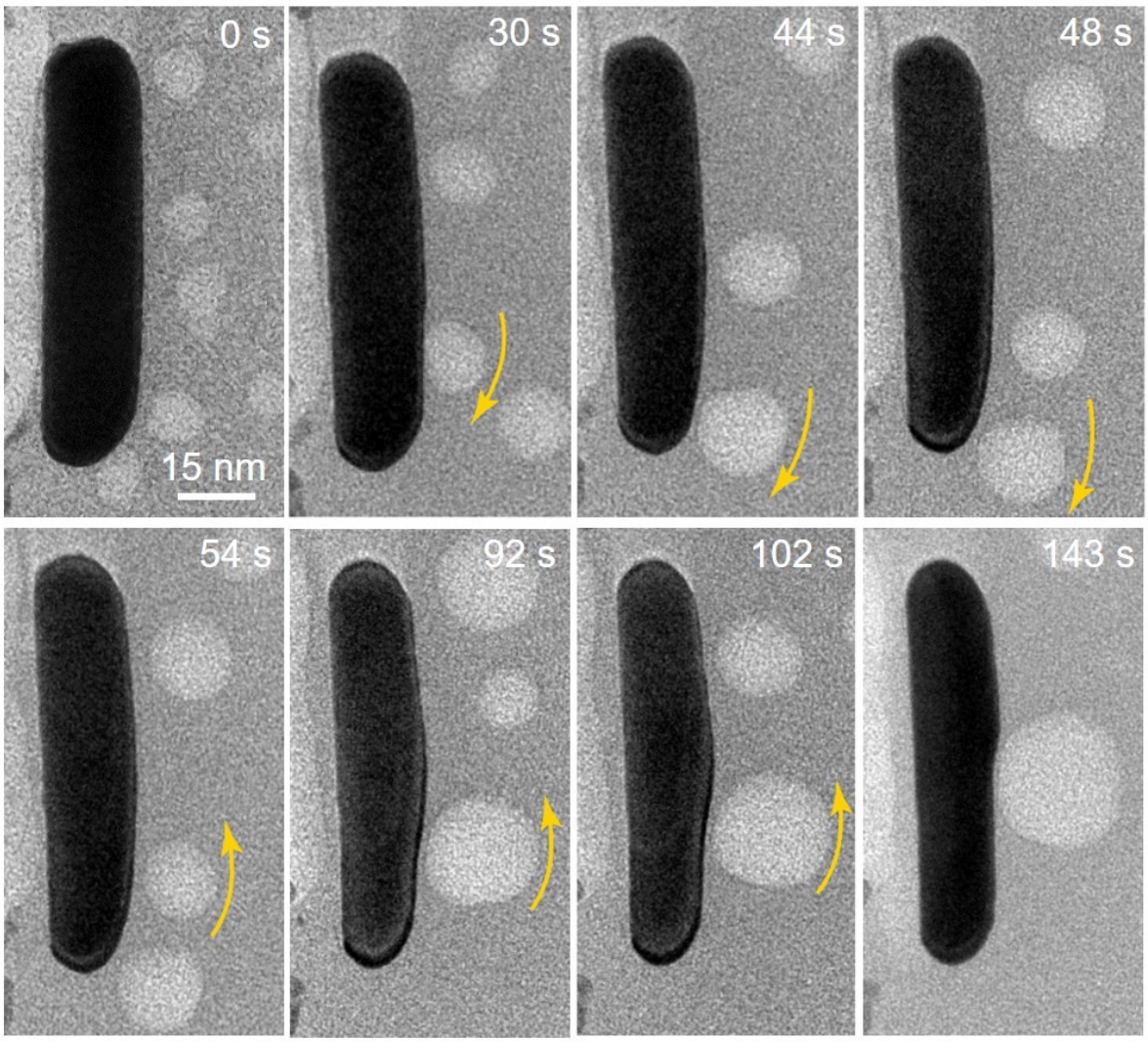

Supplementary Fig. 13. Time sequential TEM micrographs showing the morphology evolution of a Au nanorod with the presence of gas nanobubbles. The yellow arrows indicate the moving directions of the nanobubble near the Au nanorod surface. With the movement of the nanobubbles, The Au nanorod surface that is closest to the nanobubble exhibits the accelerated etching.

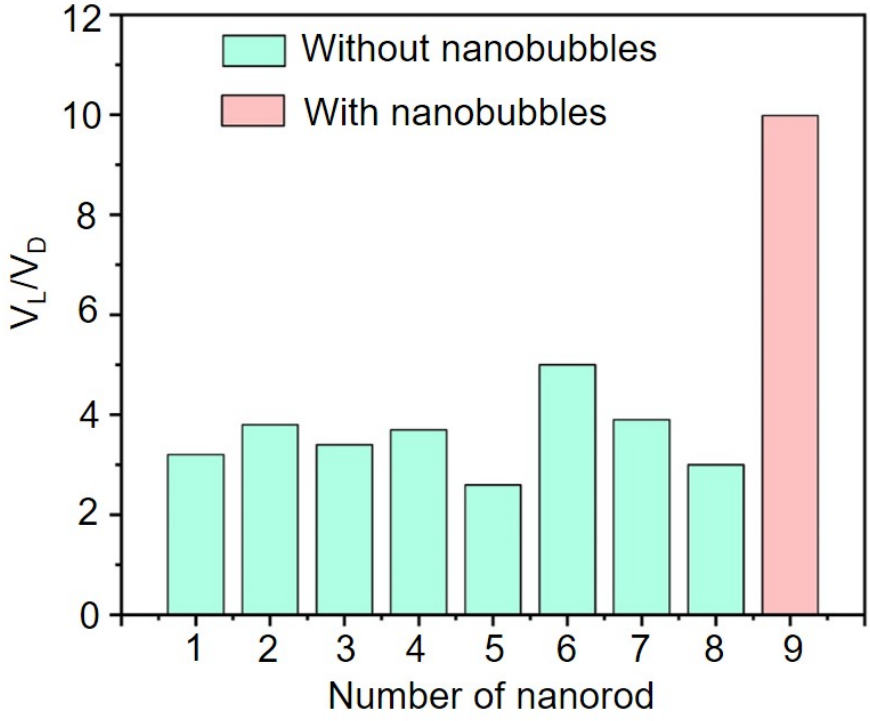

Supplementary Fig. 14. Ratios of average longitudinal and transverse etching rate (V_L/V_D) of a Au nanorod without nanobubbles (in green) and with a nanobubble at top (see image in Fig. 3).

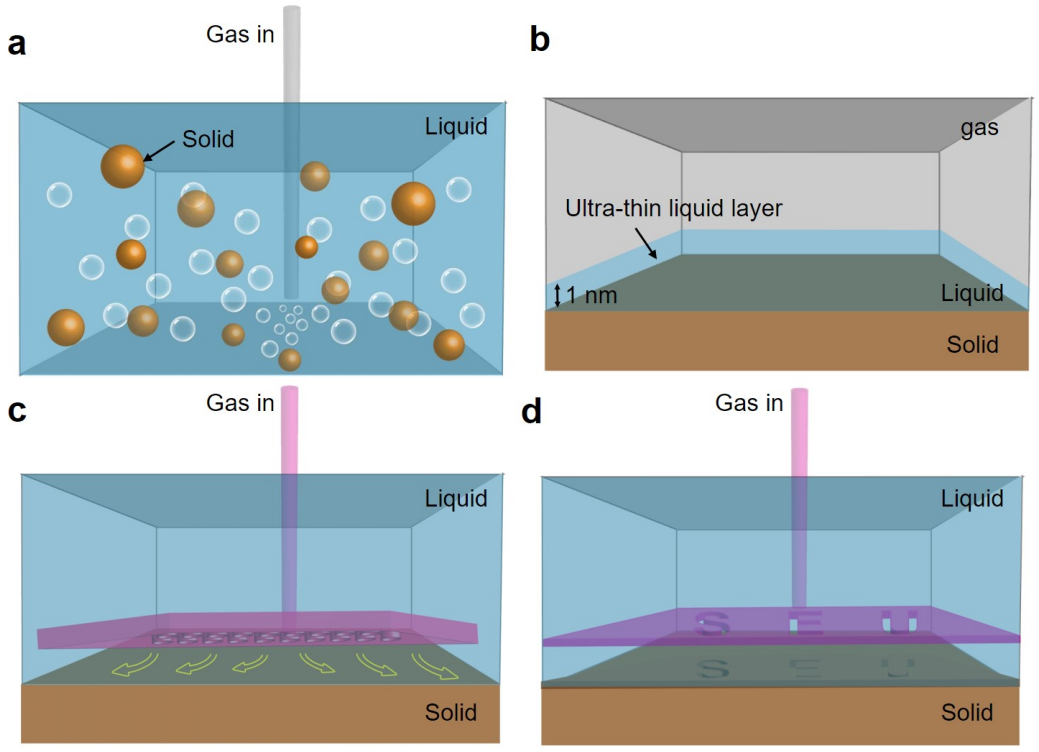

Supplementary Fig. 15. Promising strategies for accelerating the triple-phase reaction in different scenarios. a, Ultra-thin liquid layer between gas and solid particles created by continuously bubbling gas reactant to the liquid. **b**, Ultra-thin liquid layer (<1 nm) created on the surface of the solid reactant. **c**, Schematic of introducing gas reactants to the surface of a fixed solid reactant through a venting array. **d**, Schematic of the gas-liquid etching of solid materials realized by using a gas vent with a specific shape.